

Recoil distance lifetime measurements in ^{118}Xe I. M. Govil,¹ A. Kumar,¹ Hema Iyer,¹ P. Joshi,¹ S. K. Chamoli,¹ Rakesh Kumar,² R. P. Singh,² and U. Garg³¹*Department of Physics, Panjab University, Chandigarh-160014, India*²*Nuclear Science Centre, New Delhi-110067, India*³*Department of Physics, University of Notre Dame, Notre Dame, Indiana 46556*

(Received 15 October 2001; revised manuscript received 13 June 2002; published 30 December 2002)

Lifetimes of the excited states of the ground state band in ^{118}Xe are newly measured using the recoil-distance Doppler-shift technique. The reaction $^{93}\text{Nb}(^{29}\text{Si}, p3n)^{118}\text{Xe}$ at a beam energy of 135 MeV was used for this experiment. The lifetimes of the 2^+ , 4^+ , 6^+ , 8^+ , and 10^+ states of the ground state band were extracted using the computer code LIFETIME which includes the corrections due to the side feeding and the nuclear deorientation effects. The present $B(E2)$ values are in good agreement with the extracted $B(E2)$ values from the Hartee-Fock-Bogoliubov calculations. The measured $B(E2)$ values are also compared with the standard algebraic and the geometrical models. The $B(E2)$ values for the 2^+ state for this nucleus and the other Xe nuclei as a function of the neutron number are well reproduced in the framework of the algebraic model IBA-1 with O(6) symmetry and the geometrical finite range droplet model.

DOI: 10.1103/PhysRevC.66.064318

PACS number(s): 21.10.Tg, 27.60.+j

I. INTRODUCTION

The xenon nuclei have four protons out side the $Z=50$ shell closure. Their low lying levels include a series of collective even parity states. Various algebraic and the geometrical models have been used to reproduce the energies and the $B(E2)$ values for these states. The $B(E2)$ transitions provide a valuable information about their intrinsic quadrupole moment and hence the deformation of the nucleus. According to the standard models, a small but gradual increase in the xenon $B(E2)$ values is expected as the neutron number is decreased from $N=82$ to the midshell $N=66$, a flattening at the midshell, and finally a gradual decrease below $N=66$. Instead, the recent experimental values for the midshell xenon isotopes constitute a small peak [1,2]. To reproduce these newly measured $B(E2)$ values several models have been predicted. In the framework of the IBM-2, the experimental values are reproduced without the Pauli's blocking effects [3]. In the fermion dynamic symmetry model (FDSM) [4], the group structure has to be changed from O(5) to O(6) while going from the heavier ^{124}Xe ($N \geq 70$) isotopes to the lighter ^{120}Xe ($N \leq 66$) isotopes. The nucleus ^{118}Xe with $N=64$ lie below the midshell $N=66$ and according to the existing theoretical models a downward slope of the $B(E2)$ value for the 2^+ state is expected for this nucleus. We have therefore measured the lifetimes of the excited states of the ground state band of ^{118}Xe nucleus to examine critically the existing models. Our measured value for the 2^+ state is in close agreement with the value measured by Katou *et al.* [5] while the value of the 4^+ state differs significantly. We have compared our results with the theoretical predictions based on the Hartee-Fock-Bogoliubov (HFB) calculations alongwith the standard algebraic and geometrical models.

II. EXPERIMENT

Lifetimes were measured in ^{118}Xe nucleus via recoil distance method (RDM), using the reaction

$^{93}\text{Nb}(^{29}\text{Si}, p3n)^{118}\text{Xe}$. The 135-MeV ^{29}Si beam was delivered by the 15UD pelletron accelerator at Nuclear Science Centre (NSC), New Delhi. The experiment was performed using the NSC recoil distance plunger device and the Gamma Detector Array (GDA). A 1-mg/cm²-thick target of ^{93}Nb was stretched and mounted on the RDM device. The stopper was 7-mg/cm² gold foil stretched in the similar way and mounted opposite to the target. The distance between the target and the stopper (d) was calibrated using capacitance measurement method. A graph between $1/C$ and the distance (d) was plotted to get the minimum distance between the target and stopper which was found to be 10 μm . The data were acquired at target-stopper distances ranging from 10 to 10 000 μm . The larger distance (10 000 μm) was selected to see the effect of any long lived lifetime present in the decay of this nucleus which sometime affects the measurements if not properly taken care of. The gamma rays were detected with 12 Compton suppressed HPGe detectors of the Gamma Detector Array (GDA) of the NSC, New Delhi arranged in three different rings of four detectors each, and making an angle of 144°, 98°, and 50° with respect to the beam direction. A 14-element BGO multiplicity filter was used with seven detectors each at the top and the bottom of the scattering chamber. The data from any of the HPGe detectors was acquired in coincidence with the multiplicity of two from the BGO detectors. This reduces the background due to the Coulomb excitation and other unwanted γ rays due to radioactivity, etc. The HPGe detectors at a particular angle were gain matched in the software and the data were added.

III. RESULTS AND DATA ANALYSIS

Figure 1 shows the typical shifted and the unshifted peaks of $2^+ - 0^+$ (337.5 keV), $4^+ - 2^+$ (472.8 keV), $6^+ - 4^+$ (586.4 keV), $8^+ - 6^+$ (676.4 keV) and $10^+ - 8^+$ (743.0 keV) transitions at the forward angle of 45° for three target to stopper distances. The program LIFETIME [6] was used for the present analysis to fit the experimental decay curves to extract the lifetimes of the various transitions. All such curves were fit-

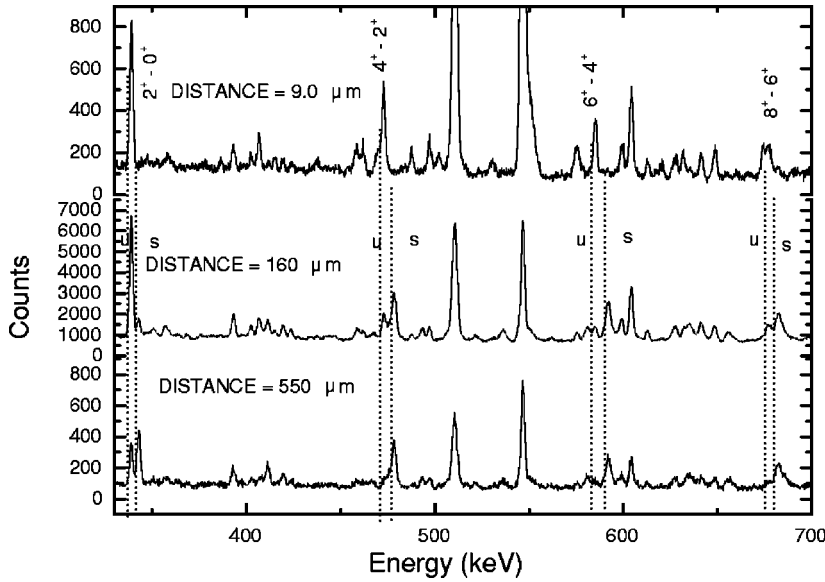


FIG. 1. Typical spectra at $+50^\circ$ with respect to beam line for different target to stopper distances.

ted with a combination of exponential functions and the lifetime for each level was extracted from these fits. The program LIFETIME includes the corrections due to the changing position of the recoiling nucleus along the flight path and the velocity-dependent solid angle. The solid angle for the shifted component is averaged along the flight path. The corrections are also made for the changes in the angular distribution due to the attenuation from the nuclear alignment. Although the hyperfine interactions occur during flight, the effect on the Doppler-shifted peak is reduced by integration over the flight time. The alignment attenuation is assumed to stop when the recoil enters the stopper. Inside the stopper large charge-exchange phenomena cause the ions to change the charge states rapidly, decoupling the hyperfine field, thereby freezing the perturbed alignment of the ions until they decay. The angular distribution of radiation from aligned nucleus can be written as

$$W(t) = 1 + A_2(t)P_2(\cos \theta) + A_4(t)P_4(\cos \theta), \quad (1)$$

where A_2 and A_4 are the angular distribution coefficients. According to Abragam and Pound [7], the attenuation can be described

$$A_2(t) = A_{20}e^{-t/\tau_2}, \quad A_4(t) = A_{40}e^{-t/\tau_4}, \quad (2)$$

where τ_2 (30.0 ps) and τ_4 (10.0 ps) are the electronic relaxation times and $A_{20} = 0.368$ and $A_{40} = -0.112$ for a completely aligned nucleus calculated at $J_0 = 50$. It is well known that only states of low spin are significantly perturbed by the atomic interactions. A correction is also made to include the gamma-ray intensity emitted while the recoils are slowing down in stopper. This intensity would lie between the shifted and the unshifted peaks. Since the flight distance and therefore the flight time is measured to the front surface of the stopper, the intensity lying between shifted and the unshifted peaks are added to the unshifted intensity.

This program also includes the corrections due to the effect of the unknown side feedings. The side feedings to all the levels were modeled to have a one step feeding and it

was ensured in analyzing the data for each γ transition that the intensities are properly balanced due to the variation of the population from the side feedings. The transition probabilities from the sidebands were adjusted to have the best fit to the experimental data. In the present analysis the top most level of the band being analyzed, was assumed to be fed by a rotational cascade comprising of five transitions of the known energies. The side feeding was found to be very small in most of the transitions therefore any systematic error due to this reason would be negligible. The quadrupole moment of this rotational band was a parameter of variation which was adjusted to have the best fit to the transition from the observed highest level. The errors were calculated by the subroutine MINUIT of the LIFETIME program which calculates the errors due to the variations of the parameters for the unit change of the chi square. Figure 2 shows the fitted decay curves for the various transitions in this nucleus. A summary of the lifetimes measured in the present work for different transitions along with the earlier results [5] are given in Table I.

In order to investigate the shape of the nucleus we have performed the total Routhian surface (TRS) calculations. The routhians were calculated using the cranked Hartree-Fock-Bogoliubov (HFB) procedure [8,9]. A rotating Woods-Saxon mean field potential along with the monopole pairing interaction was used for these calculations. The values of the pairing term Δ and the chemical potential λ were determined by solving the BCS self-consistent equations [10]. The total Routhian calculated were used for determining the microscopic corrections to the macroscopic energy using the Strutinsky procedure. Figure 3 shows the plots for the equienergy contours for the ground state band at $\hbar\omega = 0.0$ keV which predicts the minima at $\beta_2 = 0.25$. A comparison has been made in Table I between the experimental and the theoretical $B(E2)$ values extracted from the HFB calculations for different excited states. The experimental values have been calculated using the following relations:

$$B(E2; I \rightarrow I-2) = (0.0815) / [E_\gamma^5 \tau (1 + \alpha_\tau)] e^2 b^2. \quad (3)$$

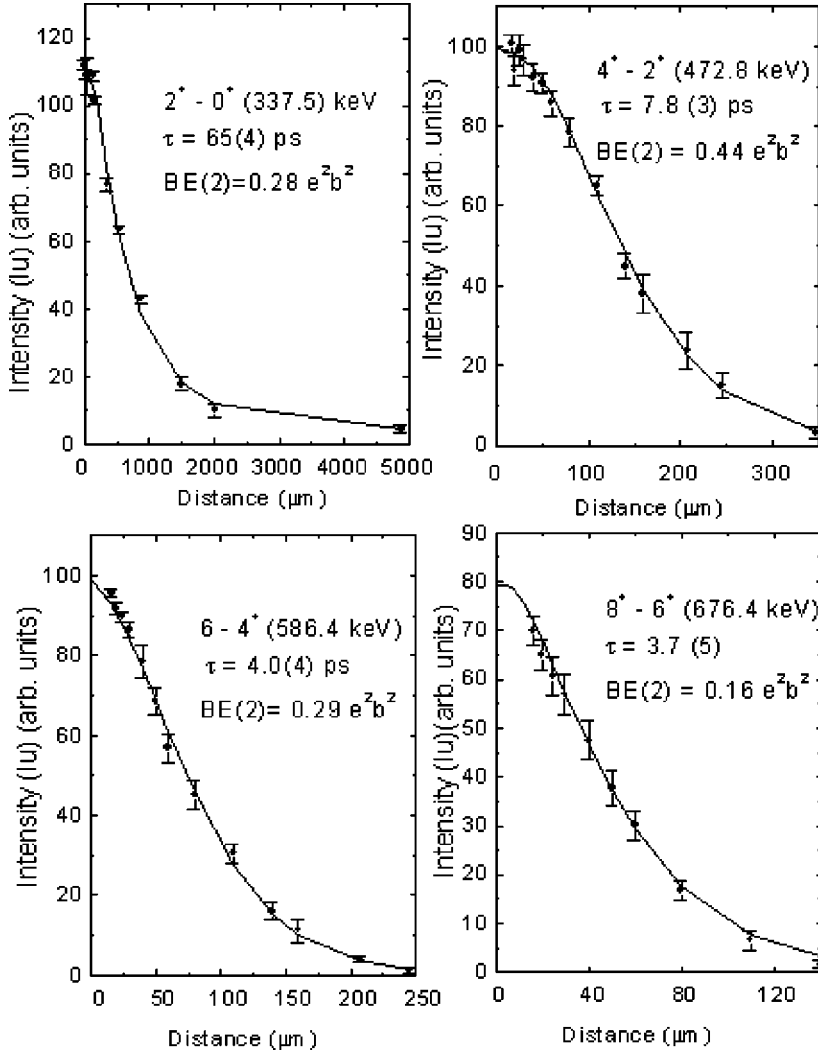


FIG. 2. Decay curves of the normalized unshifted intensities for various transitions of the ground state band in ^{118}Xe .

The theoretical Q_t and $B(E2)$ values are deduced from the β and γ values obtained from the HFB calculations and using the following relations:

$$Q_t = \sqrt{(12/5\pi)} Z e R_0^2 \beta \cos(30 + \gamma) e b, \quad (4)$$

$$B(E2; I \rightarrow I-2) = (5 Q_t^2 \langle I200 | I-20 \rangle^2) / 16 \pi e^2 b^2, \quad (5)$$

where E_γ is the energy in MeV, τ is the lifetime in ps, α_τ is the total conversion coefficient, and R_0 is the radius ($1.2 A^{1/3}$). The deformation parameter β and the triaxiality parameter γ are predicted by HFB calculations at certain

value of $\hbar\omega$. Z and A represent the atomic number and the atomic mass, respectively. Our measured values are in close agreement with HFB calculations up to 6^+ state of the ground state band.

The excitation energies and the $B(E2)$ values in the ground state band are calculated using the algebraic model IBA-1 [11] with the Hamiltonian

$$H = \varepsilon \cdot n_d + kQ \cdot Q + k'L \cdot L + k''P \cdot P, \quad (6)$$

where

TABLE I. Comparison of measured lifetimes and $B(E2)$ values for ^{118}Xe .

Transition	E (keV)	τ (ps) (Present)	τ (ps) (Ref. [5])	$\hbar\omega$ (keV)	$B(E2)$ (Present)	$B(E2)$ (HFB)
$2^+ - 0^+$	337.5	65(4)	65(3)	150	0.28(2)	0.26
$4^+ - 2^+$	472.8	7.8(3)	10.8(2)	250	0.44(2)	0.42
$6^+ - 4^+$	586.4	4.0(4)	4.6(9)	300	0.29(3)	0.32
$8^+ - 6^+$	676.4	3.7(5)	4.0(14)	350	0.16(2)	0.40
$10^+ - 8^+$	742.2	≤ 3.0	≤ 1.7	400	≥ 0.12	0.41

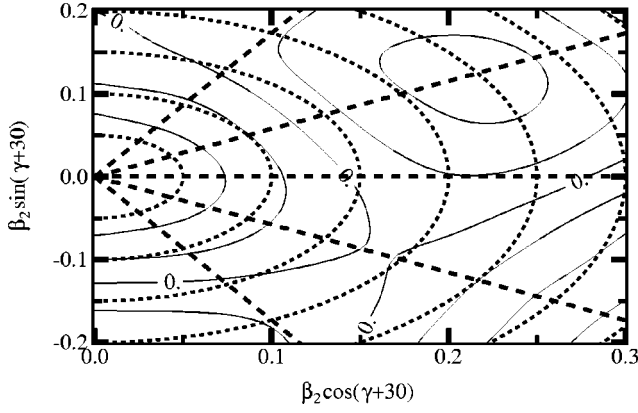


FIG. 3. Plots of the equienergy contours for the ground state band in ^{118}Xe at $\hbar\omega=0.0$ keV.

$$Q = (d^+s + s^+d) + \chi(d^+d). \quad (7)$$

In case of SU(5) symmetry, $k=0$ and for O(6) symmetry, $\chi=0$. Figure 4(a) shows the comparison of the experimental excitation energies of the excited states in the ground state band with the calculated energies from IBA-1 assuming SU(5) and O(6) symmetries. The experimental energies are well reproduced in both SU(5) and O(6) symmetries.

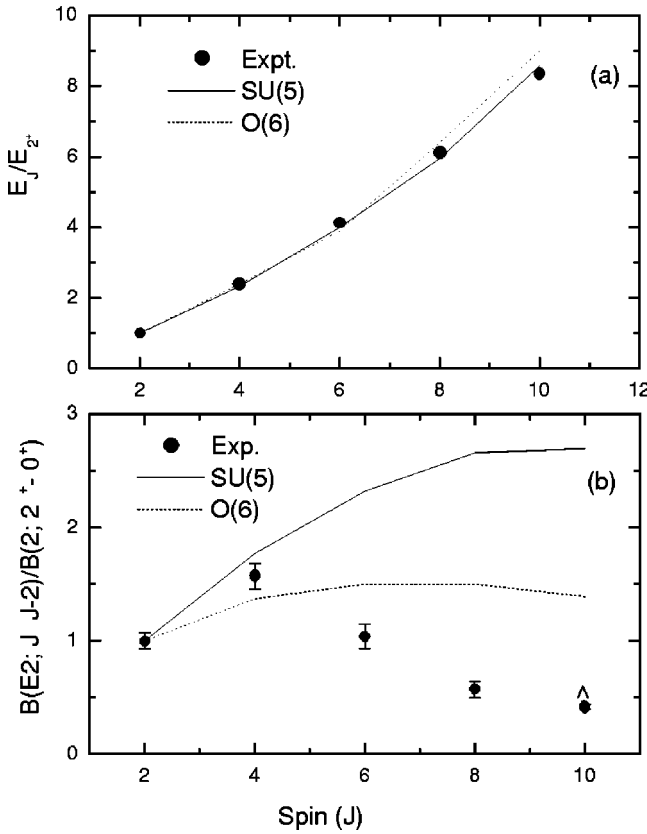


FIG. 4. A comparison of (a) the experimental E_J^+/E_2^+ ratio in ^{118}Xe isotopes with the predictions of IBA-1 with O(6) and SU(5) symmetries. (b) the experimental $B(E2)$ values for the excited states of the ground state band with IBA-1 model using O(6) and SU(5) symmetries.

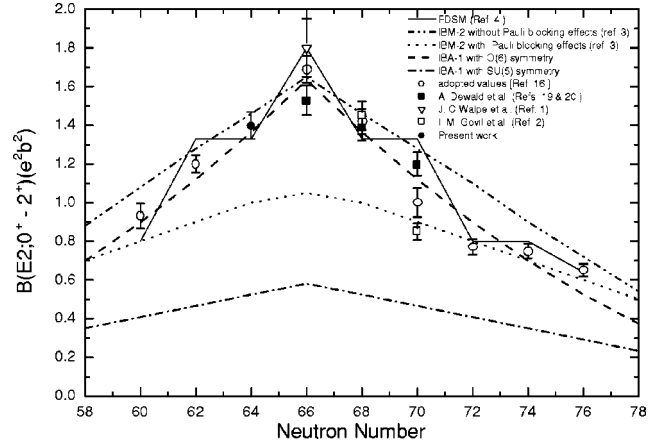


FIG. 5. A comparison of the experimental $B(E2)$ values for the lowest $2^+ - 0^+$ state in Xe isotopes with the theoretical predictions from the different algebraic models.

The $B(E2)$ values for the excited states in the ground state band are calculated in the IBA-1 model with O(6) symmetry using the relation

$$B(E2; L+2 \rightarrow L) = e_B^2 (L+2)(2N_B - L) \times (2N_B + L + 8) / 8(L+5) \quad (8)$$

and with SU(5) symmetry using the relation

$$B(E2; L+2 \rightarrow L) = e_B^2 (L+2)(2N_B - L) / 4, \quad (9)$$

where e_B is the effective boson charge and $N_B=9$ are total number of s and d bosons. The effective boson charge e_B is calculated using the experimental $B(E2; 2^+ \rightarrow 0^+)$ value and the relations for the O(6) and SU(5) symmetries as follows:

$$\text{O(6)}: e_B^2 = 5B(E2; 2^+ \rightarrow 0^+) / N_B(N_B + 4), \quad (10)$$

$$\text{SU(5)}: e_B^2 = B(E2; 2^+ \rightarrow 0^+) / N_B. \quad (11)$$

The experimental and theoretical $B(E2)$ values for ^{118}Xe from the IBA-1 normalized to $B(E2; 2^+ \rightarrow 0^+)$ for the ground state band up to 10^+ state assuming SU(5) and O(6) symmetries are compared in Fig. 4(b). The experimental $B(E2)$ values for $I \geq 6$ are found to be lower in the ^{118}Xe as compared to the theoretical predictions which is in agreement with the observations by Degraff *et al.* [12] in case of $^{114,116}\text{Xe}$ nuclei.

The experimental $B(E2)$ values for lowest $2^+ \rightarrow 0^+$ state for this nucleus along with the $B(E2)$ values for other nuclei are compared with the algebraic models in Fig. 5. The IBA-1 model with O(6) symmetry reproduces very well the experimental $B(E2)$ values of the broad range of Xe isotopes. However, the experimental values do not support the SU(5) symmetry. In both the calculations, effective charge $e_B = 0.108$ is used. The ratio E_4^+/E_2^+ for Xe isotopes, which peaks at a value of 2.5 in the midshell region corresponding to the γ -soft O(6) limit and decreases towards 2.0 at neutron number approaching $N=82$ corresponding to the vibrational

SU(5) limit, suggests a gradual change in the structure. According to D. Feng *et al.* [13], in Xe isotopes switching from the vibrational SU(5) symmetry for $N \geq 72$ to the γ -soft O(6) symmetry for $N \leq 70$ produces a sharp discontinuity. Casten *et al.* [14] have also argued that the O(6) character is valid in the xenon-barium-cerium region for $N \leq 76$. The other indicators such as the energy of the 2^+_{γ} state also support this γ -soft rotor model for the xenon isotopes.

In the framework of IBA-2, Otsuka *et al.* [3] have attempted to describe the systematic behavior of the $B(E2)$ values for the even-even Xe, Ba, and Ce nuclei assuming the SU(5) symmetry. They were particularly interested with apparent saturation of the $B(E2)$ strength as the midshell is approached. They reproduced the experimental $B(E2)$ values very well for $N \geq 70$ xenon isotopes with Pauli blocking effect, however, for the more deformed midshell xenon isotopes ($N \leq 70$), where the dominant symmetry is O(6), there is a marked underprediction. They have shown that adding the Pauli blocking to $E2$ transition operator in IBA-2 does provide saturation for the ytterbium isotopes and some saturation near $N=66$ in the xenon isotopes. On the other hand, the calculations with IBA-2 without Pauli blocking effects are in agreement with the results of the recent experiments. The fermion dynamical symmetry model (FDSM) predicts the saturation for the ytterbium isotopes but no saturation for the xenon isotopes. In the FDSM calculations [4] the experimental $B(E2)$ values for the midshell isotopes are in good agreement with the O(6) symmetry. Our present $B(E2)$ value ($2^+ \rightarrow 0^+$) for ^{118}Xe isotope is in good agreement with the FDSM, IBA-1 with O(6) symmetry, and IBA-2 without Pauli blocking effects as shown in Fig. 5.

Raman *et al.* [15,16] have extensively compared the $B(E2)$ values for the Xe isotopes with different geometrical

models, e.g., single-shell asymptotic Nilsson model (SSANM) [16], finite range droplet model (FRDM) [17], Hartree-Fock calculations [18]. The FRDM and Hartree-Fock calculations give a better agreement with our measurement as compared to the single shell Nilsson asymptotic model [19,20].

IV. SUMMARY

Lifetimes of the ground state band up to 10^+ state in ^{118}Xe nucleus have been measured with the recoil-distance technique. Our measured value of the lifetime for the 4^+ state differs from the earlier measurement of T. Katou *et al.* while for other states our values are in agreement with their values within experimental errors. The present $B(E2)$ values for the $I < 6$ excited states are consistent with the theoretical $B(E2)$ values extracted from the Hartree-Fock-Bogoliubov (HFB) calculations and IBA-1 calculations. A band crossing is therefore expected at $I \geq 6^+$. The $B(E2)$ values for the lowest $2^+ - 0^+$ transition in ^{118}Xe nucleus along with the other Xe nuclei agree very well with the FDSM and the IBA-1 calculations with O(6) symmetry. In the geometrical models, the FRDM and multishell Hartree-Fock calculations give a better agreement as compared to the single shell Nilsson asymptotic model.

ACKNOWLEDGMENTS

The authors wish to thank the crew of the Nuclear Science Centre, New Delhi, for providing an excellent beam of ^{29}Si during the course of the experiment. We are also thankful to UGC-NSC and NSF-USA (Grant Nos. phy 99-01133 and Int-0115336 for the financial support needed for this work.

-
- [1] J. C. Walpe, B. F. Davis, S. Naguleswaran, R. Revoil, and U. Garg, *Phys. Rev. C* **52**, 1792 (1995).
 - [2] I. M. Govil, A. Kumar, H. Iyer, H. Li, U. Garg, S. S. Ghugre, T. Johnson, R. Kaczarowski, B. Kharraja, S. Naguleswaran, and J. C. Walpe, *Phys. Rev. C* **57**, 632 (1998).
 - [3] T. Otsuka, X. W. Pan, and A. Arima, *Phys. Lett. B* **247**, 191 (1990).
 - [4] C. L. Wu, D. H. Feng, and M. W. Guidry, in *Advances in Nuclear Physics*, edited by J. W. Negel and E. Vogt (Plenum, New York, 1994), Vol. 21, p. 227.
 - [5] T. Katou, Y. Tendow, H. Kumagai, Y. Gono, and A. Hashizume, *Proceedings of the International Conference on Nuclear Physics, Berkeley, 1980*, p. 751.
 - [6] J. C. Wells *et al.*, ORNL/TM-9105, 1985.
 - [7] A. Abragam and R. V. Pound, *Phys. Rev.* **92**, 943 (1953).
 - [8] P. Ring and P. Schuck, *The Nuclear Many Body Problem* (Springer-Verlag, Berlin, 1980), p. 244.
 - [9] W. Nazarewicz, M. A. Rieley, and J. D. Garrett, *Nucl. Phys.* **A512**, 61 (1990).
 - [10] S. G. Nilsson and I. Ragnarsson, *Shapes and Shells in Nuclear Structure* (Cambridge University Press, Cambridge, England, 1995), p. 290.
 - [11] J. B. Gupta (private communication).
 - [12] J. DeGraff, M. Cromaz, T. E. Drank, V. P. Janzen, R. C. Radford, and D. Ward, *Phys. Rev. C* **58**, 164 (1998).
 - [13] D. H. Feng, C. L. Wu, M. W. Guidry, and Z. P. Li, *Phys. Lett. B* **205**, 156 (1988).
 - [14] R. F. Casten *et al.*, *Phys. Lett.* **152B**, 22 (1985).
 - [15] S. Raman, J. A. Seikh, and K. H. Bhatt, *Phys. Rev. C* **52**, 1380 (1995).
 - [16] S. Raman *et al.*, *At. Data Nucl. Data Tables* **78**, 1 (2001).
 - [17] P. Moller and J. R. Nix, *Nucl. Phys.* **A536**, 20 (1992).
 - [18] N. Tajima, N. Onishi, and S. Takahara (private communication).
 - [19] A. Dewald, S. Harissopoulos, and P. Von Brentano, *Z. Phys. A* **334**, 163 (1989).
 - [20] A. Dewald *et al.*, *Proceedings of the Zakopane School on Physics, Poland, 1990*, Vol. 2.